Published online 30 March 2012 Nucleic Acids Research, 2012, Vol. 40, No. 13 6135–6143
doi:10.1093/nar/gks273

TricycloDNA-modified oligo-2′-deoxyribonucleotides reduce scavenger receptor B1 mRNA in hepatic and extra-hepatic tissues—a comparative study of oligonucleotide length, design and chemistry

Sue Murray[1], Damian Ittig[2], Erich Koller[1], Andres Berdeja[1], Alfred Chappell[1], Thazha P. Prakash[1], Michaela Norrbom[1], Eric E. Swayze[1], Christian J. Leumann[2,*] and Punit P. Seth[1,*]

[1]Isis Pharmaceuticals, Inc., 2855 Gazelle Court, Carlsbad, CA 92010, USA and [2]Department of Chemistry and Biochemistry, University of Bern, Freiestrasse 3, CH-3012 Bern, Switzerland

Received December 5, 2011; Revised March 9, 2012; Accepted March 12, 2012

ABSTRACT

We report the evaluation of 20-, 18-, 16- and 14-mer phosphorothioate (PS)-modified tricycloDNA (tcDNA) gapmer antisense oligonucleotides (ASOs) in T_m, cell culture and animal experiments and compare them to their gap-matched 20-mer 2′-*O*-methoxyethyl (MOE) and 14-mer 2′,4′-constrained ethyl (cEt) counterparts. The sequence-matched 20-mer tcDNA and MOE ASOs showed similar T_m and activity in cell culture under free-uptake and cationic lipid-mediated transfection conditions, while the 18-, 16- and 14-mer tcDNA ASOs were moderate to significantly less active. These observations were recapitulated in the animal experiments where the 20-mer tcDNA ASO formulated in saline showed excellent activity (ED_{50} 3.9 mg/kg) for reducing SR-B1 mRNA in liver. The tcDNA 20-mer ASO also showed better activity than the MOE 20-mer in several extra-hepatic tissues such as kidney, heart, diaphragm, lung, fat, gastrocnemius and quadriceps. Interestingly, the 14-mer cEt ASO showed the best activity in the animal experiments despite significantly lower T_m and 5-fold reduced activity in cell culture relative to the 20-mer tcDNA and MOE-modified ASOs. Our experiments establish tcDNA as a useful modification for antisense therapeutics and highlight the role of chemical modifications in influencing ASO pharmacology and pharmacokinetic properties in animals.

INTRODUCTION

Over the recent years, chemically modified oligonucleotides have been extensively investigated as potential drugs (1). Currently, more than 30 candidates are in clinical trials targeting a large variety of diseases including cancer, metabolic diseases and genetic disorders. Mipomersen, a second generation antisense oligonucleotide that targets apolipoprotein B, has shown impressive reductions in serum apolipoprotein B, LDL-cholesterol and other atherogenic lipids in multiple phase III clinical trials (2). The general mode of action of antisense oligonucleotides is based on specific Watson–Crick recognition of target RNAs, which results in modulation of the function of the target RNA. In the original antisense approach, a single-stranded oligonucleotide targets a mRNA and suppresses its translation either via a steric block or by RNase H-mediated RNA degradation. Variations of steric block inhibitors include oligonucleotides that interfere with splicing of a pre-mRNA, leading to selective exon inclusion or exclusion, or alternative splicing. In addition, oligonucleotide-dependent degradation of target RNA can be induced by small double-stranded interfering RNAs (siRNAs) which guide an mRNA of interest into the RNA-induced silencing complex (RISC) where it is cleaved (3). Yet, another approach is based on targeting micro-RNAs (miRNAs) that are genetically encoded and function as natural regulators of translation, by single-stranded antisense oligonucleotides (4–6).

The specific chemical features of single-stranded antisense oligonucleotides fundamentally determine their

*To whom correspondence should be addressed. Tel: +1 760 603 2587; Fax: +1 760 603 3891; Email: pseth@isisph.com
Correspondence may also be addressed to Christian J. Leumann. Tel: +41 31 631 4355; Fax: +41 31 631 3422;
Email: christian.leumann@ioc.unibe.ch

© The Author(s) 2012. Published by Oxford University Press.
This is an Open Access article distributed under the terms of the Creative Commons Attribution Non-Commercial License (http://creativecommons.org/licenses/by-nc/3.0), which permits unrestricted non-commercial use, distribution, and reproduction in any medium, provided the original work is properly cited.

source: https://doi.org/10.7892/boris.15321 | downloaded: 12.10.2024

biological function (7). The most important factors are affinity for target RNA, biostability against nuclease degradation and bioavailabilty in animals. First generation classical antisense oligodeoxyribonucleotide phosphorothioates (PS **1**, Figure 1) elicit RNaseH activity and show increased biostability, however, their affinity to complementary RNA is moderate. On the other hand, high-affinity RNA binders such as 2′-modified RNA (8), 2′,4′-bridged nucleic acids (BNA, also known as locked nucleic acid or LNA) (9), hexitol nucleic acids (HNA) (10) or tricyclo-DNA (tcDNA) (11) do not elicit RNaseH activity when used as mixmers. To circumvent this drawback, oligonucleotide gapmers have been introduced that show a window of natural nucleotides in the center of the sequence flanked by chemically modified wings on either side (12). Such chimeric oligonucleotides combine the features of high-RNA affinity and biostability while maintaining the ability to degrade the targeted mRNA via an RNaseH mechanism.

As part of a comprehensive program aimed at elucidating the structure–activity relationships (SAR) of chemically modified ASOs in animals, we have recently reported the evaluation of RNase H active gapmer ASOs containing 2′,4′-bridged nucleic acids and hexitol analogs (13–17). tcDNA represents another oligonucleotide scaffold that exhibits favorable physico-chemical properties, such as improved target RNA affinity and nuclease stability, for the antisense approach (18,19). Yet, gapmer ASOs containing PS-modified tcDNA have not been evaluated in cellular or in animal experiments. In this light, we present here a comprehensive analysis of the biophysical, pharmacological and tissue distribution properties of 14- to 20-mer phosphorothioate tcDNA gapmer ASOs and compare them to sequence matched MOE and 2′,4′-constrained ethyl BNA (cEt) control ASOs. We show that tcDNA-modified ASOs formulated in saline show potent and robust antisense effects in hepatic as well as extra-hepatic tissues without producing toxicity and highlight the role of chemical modifications in influencing ASO pharmacology and pharmacokinetic properties in animals.

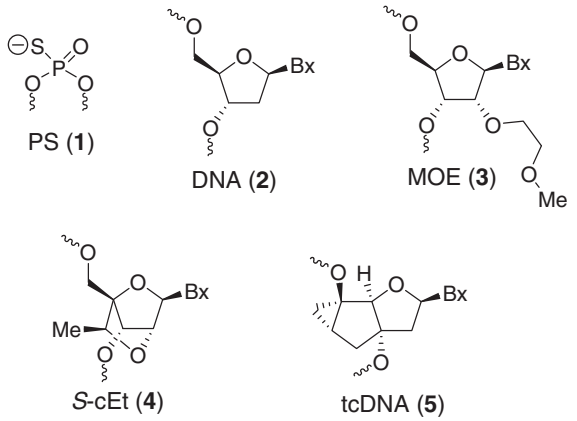

Figure 1. Structures of oligonucleotide modification evaluated in this study.

MATERIALS AND METHODS

Oligonucleotide synthesis and purification

The syntheses of the tc-DNA gapmer oligonucleotides were performed on a 10.0 μmol scale on a *Gene Assembler Plus* DNA synthesizer (Pharmacia/GE healthcare) using standard phosphoramidite chemistry. Tc-nucleoside-modified long chain alkylamino CPG (Link Technologies) was used as solid support. Tc-phosphoramidites [0.15 M in CH_3CN for T, C and G and dichloroethane (DCE) for A] were coupled with 5-(ethylthio)-1*H*-tetrazole (ETT, 0.25 M in CH_3CN) as activator with a coupling time of 12 min. Sulfurization was carried out using phenylacetyl disulfide (PADS, 0.2 M solution in dry pyridine/CH_3CN 1:1, v/v) for 3.5 min. After synthesis was completed, the support-bound oligonucleotides were treated with a solution of Et_3N/CH_3CN (1:1, v/v) for 2 h and then deprotected and detached from solid support with 33% aqueous NH_3 for 16 h at 55°C. The crude material was purified by ion-exchange HPLC (Source 30Q, GE Healthcare) with linear gradients (0–50%) of buffer B (0.1 M NH_4OAc, H_2O:CH_3CN 7:3, pH 8.0, 1.5 M NaBr) in buffer A (0.1 M NH_4OAc, H_2O:CH_3CN 7:3 pH 8.0) as eluent. Oligonucleotides were desalted over HiPrep^{TM} 26/10 columns (GE Healthcare) and lyophilized. Sequences and analytical data are summarized in Supplementary Table S1. ASOs **A5** and **A6** were synthesized according to procedures described previously (16,20).

Cells and reagents

MHT cells (21) were cultured in DMEM supplemented with 10% fetal calf serum, streptomycin (0.1 μg/ml) and penicillin (100 U/ml). ASO transfection was performed using Opti-MEM containing 5 μg/ml Lipofectamine 2000 at the indicated amount of ASO for 4 h at 37°C, as described previously (22,23).

Taqman RT–PCR

Total mRNA was isolated using a QIAGEN RNAeasy kit (QIAGEN, Valencia, CA, USA). Reduction of target mRNA expression was determined by real time RT–PCR (1) using StepOne RT–PCR machines (Applied Biosystems). The sequences used in the RT–PCR reaction are 5′-TGACAACGACACCGTGTCCT-3′ for the forward primer, 5′-ATGCGACTTGTCAGGCTG G-3′ for the reverse primer and 5′-CGTGGAGAACCG CAGCCTCCATT-3′ for the probe. The expression data were normalized to ribogreen (Invitrogen). Data are mean values ± standard deviations of three replicates. IC_{50} values were calculated using GraphPad Prism 4 software.

Protocols for animal experiments

The Institutional Animal Care and Use committee (IACUC) approved all procedures. Male Balb/c mice were housed 4/cage on a 12:12-h light/dark cycle. For the first study, tcDNA, MOE, and cEt ASO solutions were prepared in PBS and injected subcutaneously (s.c) twice a week at a concentration of 25, 5, 1 or 0.5 mg/kg for 3 weeks. For the follow-up study, mice were injected s.c at 25 mg/kg twice a week for 3 weeks. Mice were

sacrificed 48 h after the last dose. Blood samples were collected by cardiac puncture and plasma chemistries (alanine amino transferase, aspartate amino transferase, bloood urea nitrogen, total bilirubin, cholesterol and triglycerides) values were measured on the Olympus AU400 Clinical Analyzer (Beckman Coulter, CA, USA).

RNA analysis for animal experiments

Liver, kidney, diaphragm, lung, white adipose, heart, quadriceps and gastrocnemius muscle were dissected, weighed and immediately homogenized in 2 ml of PureLink RNA lysis buffer (Life Technologies, CA, USA). Total RNA was isolated using the Purlink RNA Mini Kit (Life Technologies). Reduction of target mRNA expression was determined by real time RT–PCR using 7700 RT–PCR sequence detector (Applied Biosystems). Data are mean values ± standard deviations of three replicates. The sequences used in the RT-PCR reaction are 5′-TGACAACGACACCGTGTCCT-3′ for the forward primer, 5′-ATGCGACTTGTCAGGCTGG-3′ for the reverse primer and 5′-CGTGGAGAACCGCAGCCTCC ATT-3′ for the probe. RNA transcripts were normalized to total RNA levels using RiboGreen, RNA Quantitation Reagent (Molecular Probes). RiboGreen is an ultrasensitive flourescent nucleic acid stain which when bound to RNA has a maximum excitation/emission at ~500 nm/525 nm. ED_{50} values were calculated using GraphPad Prism 4 software.

RESULTS

Oligonucleotide design considerations

The prototypical design of a second generation antisense oligonucleotide employs a 8–14 base PS-modified deoxynucleotide 'gap' flanked on either end with 2–5 MOE nucleotides (MOE gapmer) (24–26). Typically, each MOE nucleotide confers + 1–2°C/mod. towards the overall duplex thermal stability depending on the position and sequence context of the incorporation. The PS backbone promotes binding to plasma proteins thereby reducing renal excretion of the oligonucleotide (27). This allows the ASO to distribute to peripheral tissues such that one observes reproducible and robust antisense effects in animal models especially when targeting genes expressed in the liver. More recently, we and others have shown that replacing MOE with high-affinity BNA nucleotides in the 'wings' of second generation ASOs allows for the use of oligonucleotides as short as 12- to 14-mer in length (13,28). In these designs, the BNA nucleotide contributes +3–4°C/mod. towards duplex thermal stability. However, the reduced PS content of the shorter ASOs designs results in reduced exposure to peripheral tissues. Despite this, somewhat counterintuitively, these ASOs exhibit improved activity in animal experiments although antisense effects towards gene targets expressed in tissues other than liver have not been well-characterized to date. In comparison to BNA, tcDNA exhibits intermediate improvement (ΔT_m + 2–4°C/mod.) in duplex thermal stability as measured by incorporation in the interior of a phosphodiester deoxyribo-oligonucleotide (29). However, RNase H-active gapmer ASOs are typically uniformly PS modified and position the modified nucleotides in the wings where the effects of tcDNA on duplex thermal stability have not been well-characterized. Given this background, it was difficult to ascertain a priori what ASO length and tcDNA content would be optimal. As a result, we prepared the gap-matched 20-, 18-, 16- and 14-mer tcDNA (ASOs **A1–A4**, Table 1) versions of a previously identified potent 5-10-5 MOE gapmer (**A5**) targeting scavenger receptor B1 (SR-B1), a ubiquitously expressed gene whose physiological role is related to cholesterol uptake into tissues (30). The SR-B1 receptor has also been implicated as an entry point for viruses such as HCV (31) and other pathogens (32) and its down-regulation could provide a therapeutic benefit by preventing entry of infectious pathogens into host cells. In addition to the 5-10-5 MOE control, we also evaluated a gap-matched 2-10-2 14-mer cEt ASO **A6** as an additional control for the comparative study.

Table 1. Sequence, design features, T_m, activity for reducing SR-B1 mRNA in MHT cells and in mouse liver for tcDNA, MOE and cEt-modified PS gapmer ASOs

ASO	Sequence (5′to 3′)[a]	Mod.	Length	Design	Tm (°C)[b]	IC_{50} (nM)[c]	IC_{50} (nM)[d]	ED_{50} (mg/kg)e
A1	**p-GCTTC**AGTCATGACT**TCCTT**	tcDNA	20-mer	5-10-5	71.2	0.57	54.5	3.9
A2	**p-CTTC**AGTCATGACT**TCCT**	tcDNA	18-mer	4-10-4	63.9	0.73	238.0	4.5
A3	**p-TTC**AGTCATGACT**TCC**	tcDNA	16-mer	3-10-3	58.2	5.34	407.7	7.1
A4	**p-TC**AGTCATGACT**TC**	tcDNA	14-mer	2-10-2	49.7	11.58	>1000	16.4
A5	**G^{m}CTT^{m}C**AGT^{m}CATGA^{m}CT**T^{m}C^{m}CTT**	MOE	20-mer	5-10-5	69.7	0.63	45.0	3.5[f]
A6	**T^{m}C**AGT^{m}CATGA^{m}CT**T^{m}C**	*S*-cEt	14-mer	2-10-2	59.0	2.48	138.5	<1.0[g]

[a]Bold and underlined alphabet indicates modified nucleotides.
[b]T_m values were measured in 10 mM sodium phosphate buffer (pH 7.2) containing 100 mM NaCl and 0.1 mM EDTA, Sequence of RNA complement 5′-r(UUGAAAGGAAGTCATGACTGAAGC)-3′; all internucleosidic linkages in ASOs **A1–A6** are phosphorothioate except the 5′-terminal phosphate in ASOs **A1–A4**.
[c]IC_{50} values for reducing SR-B1 mRNA in MHT cells after transfection of ASO with lipofectamine.
[d]IC_{50} values for reducing SR-B1 mRNA in MHT cells under free-uptake conditions.
[e]ED_{50} values for reducing SR-B1 mRNA in mouse liver.
[f]ED_{50} values obtained from a different experiment.
[g]Estimated ED_{50} based on reduction of SR-B1 mRNA (54 ± 6.6% at 1 mg/kg dose) observed in this study. See Supplementary Figures S1, S2, S4 and S5 for dose–response curves.

Duplex thermal stability measurements of modified ASOs with RNA

We first evaluated all the ASOs in thermal stability experiments using a 24-mer RNA complement (Table 1). We chose the longer complement since the biological target for these ASOs, i.e. the mRNA, is not length matched to the ASOs (33). As would be expected, increasing the length and tcDNA content in the modified ASOs led to increases in duplex thermal stability. However, somewhat surprisingly, the increase in affinity was highly dependent on the context of the incorporation. For example, the 14-mer 2-10-2 tcDNA ASO **A4** showed a T_m of 49.7°C, but the T_m of the 16-mer 3-10-3 ASO **A3** was 58.2°C, corresponding to a ΔT_m of +4°C for each of the added nucleotide. For the 18-mer 4-10-4 (T_m 63.9°C) and the 20-mer 5-10-5 (T_m 71.2°C) tcDNA ASOs **A2** and **A1**, respectively, each tcDNA nucleotide contributed roughly +2.5°C and +3.5°C, respectively, towards the increase in overall duplex thermal stability. In comparison, the T_m of the 5-10-5 MOE and the 2-10-2 cEt ASOs **A5** and **A6** were 69.7 and 59.0°C, respectively. It should be noted that ASOs **A5** and **A6** were synthesized using 5-Me groups (ΔT_m + 0.5°C/mod.) (34) on the cytosine nucleobases in the gap and in the wings (6 for MOE ASO **A5** and 4 for cEt ASO **A6**) while the tcDNA ASOs were not. Thus, it is anticipated that, if needed, the RNA affinity of the tcDNA ASOs can be further increased by introducing 5-Me groups on the cytosine nucleobases.

Cell culture evaluation of ASOs A1–A6

We next evaluated all the ASOs in MHT cells under free-uptake conditions and with cationic lipid transfection to deliver the oligonucleotides (21). Using cationic lipid transfection, all the tcDNA ASOs showed activity in cell culture consistent with their duplex thermostability measurements (Table 1 and Supplementary Figure S1). The 20-mer tcDNA ASO **A1** had the highest T_m and showed the best activity in cell culture (IC_{50} = 0.57 nM), followed by the 18-mer ASO **A2** (IC_{50} = 0.73 nM), 16-mer ASO **A3** (IC_{50} = 5.34 nM) and the 14-mer ASO **A4** (IC_{50} = 11.6 nM). Also consistent with the T_m data, the 5-10-5 MOE ASO **A5** (IC_{50} = 0.63 nM) showed activity comparable to 20-mer tcDNA ASO **A1**. The 14-mer cEt ASO **A6** showed ~5-fold reduced activity (IC_{50} = 2.48 nM) relative to the 20-mer tcDNA or MOE ASO **A1** and **A5**, respectively. However, the activity of ASO **A6** was 2-fold better than that of the 16-mer tcDNA ASO **A3** even though both the ASOs had almost identical T_m.

In the absence of the cationic lipid transfection, all the ASOs showed almost 100-fold reduction in activity but the overall potency trends were similar to those observed in the transfection assay (Table 1 and Supplementary Figure S2). In the tcDNA series, the 20-mer ASO **A1** showed the best activity (IC_{50} = 55 nM) followed by **A2** (IC_{50} = 238 nM) and **A3** (IC_{50} = 408 nM), while **A4** showed very poor activity (IC_{50} > 10 000 nM). As before, the MOE 20-mer ASO **A5** (IC_{50} = 45 nM) showed activity comparable to ASO **A1** while the 14-mer cEt ASO **A6** (IC_{50} = 139 nM) was ~3-fold less active. Once again, ASO **A6** showed 3-fold better activity as compared to the 16-mer ASO **A3** despite similar overall T_m.

We also measured oligonucleotide copy numbers in each cell to ascertain if ASOs with different lengths and chemical modifications in the flanks were taken up differentially into MHT cells under free-uptake conditions (Supplementary Figure S3). Somewhat surprisingly, we found that all the tcDNA ASOs showed very similar uptake into MHT cells irrespective of oligonucleotide length. Thus, it appears that introducing more than four tcDNA monomers into an ASO does not increase cellular uptake or accumulation, but the increased tcDNA content is required to boost RNA affinity to produce an antisense effect. In contrast to the tcDNA ASOs, the MOE and cEt ASOs **A5** and **A6**, respectively, showed almost 2-fold lower ASO copy numbers/cell. Thus, the improved activity of the cEt ASO **A6** relative to the tcDNA 14-mer, 16-mer or the 18-mer ASOs cannot be explained by increased uptake of this ASO into MHT cells under free-uptake conditions.

Evaluation of ASOs A1–A6 in animal experiments

We next evaluated the ASOs **A1–A6** in animal experiments. Mice (n = 4/group) were injected sub-cutaneously (s.c.) with 0.5, 1.0, 5.0 and 25.0 mg/kg of tcDNA ASOs, 5 and 25 mg/kg of MOE ASO **A5** and 1 and 25 mg/kg of cEt ASO **A6** formulated in saline twice a week for 3 weeks (Figure 2). While the MOE and cEt ASOs **A5** and **A6** were only evaluated at two doses in this study, ASO **A5** was previously evaluated in a separate dose-reponse experiment where it showed good potency (ED_{50} = 3.5 mg/kg; Supplementary Figure S4). While a complete dose–response for the cEt ASO **A6** is not available, the ED_{50} can be estimated (ED_{50} < 1 mg/kg) based on the reduction of SR-B1 mRNA (54 ± 6.6% at the 1 mg/kg dose) observed in this study (Table 1). The animals were sacrificed 48 h after the last ASO dose and the SRB1 mRNA in liver was measured by quantitative RT–PCR and normalized to the saline treated group (Figure 2A and Supplementary Figure S5). In addition, we also recorded other parameters, such as plasma transaminases and organ weights, as gross indicators of ASO tolerability. As seen in the cell culture experiments, the tcDNA ASOs showed dose-dependent reductions of the SR-B1 mRNA in liver with the 20-mer **A1** exhibiting the best potency (ED_{50} = 3.9 mg/kg) followed by the 18-mer **A2** (ED_{50} = 4.5 mg/kg), 16-mer **A3** (ED_{50} = 7.1 mg/kg) and 14-mer **A4** (ED_{50} = 16.4 mg/kg). Thus, in the tcDNA length series, the animal experiments recapitulated the potency trend observed in the free-uptake cell culture study even though the magnitude of the potency difference was not similar.

To see if the activity seen in liver could be extended to other tissues, we also measured the down-regulation of SR-B1 mRNA in quadriceps and heart muscle (Figure 2B and C). Once again, we observed dose-dependent reductions in SR-B1 mRNA in both heart and quadriceps although the potency relative to liver was reduced for all the ASOs tested. The down-regulation of SR-B1 gene expression results in an increase in the

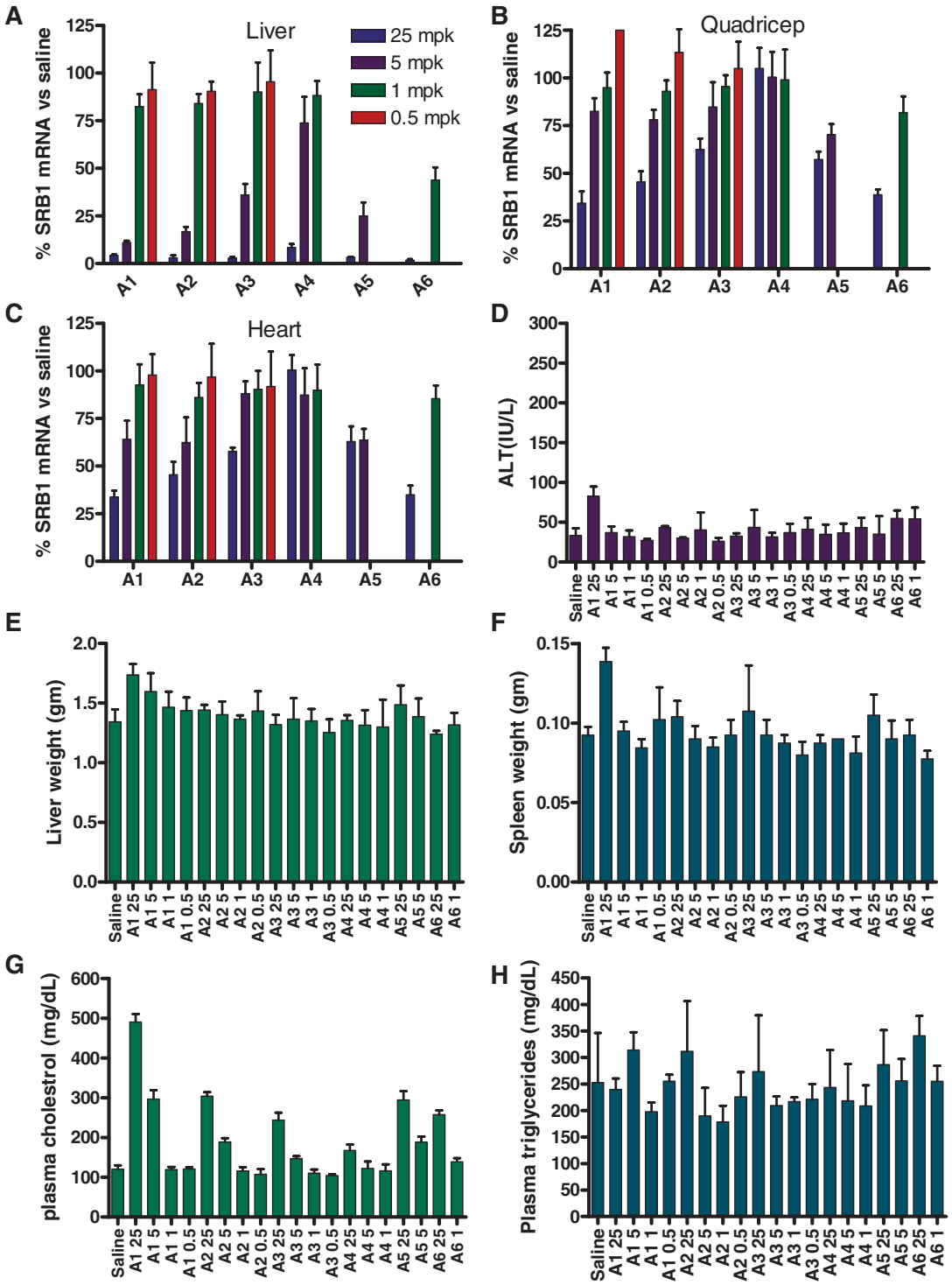

Figure 2. Reduction of SR-B1 mRNA and tolerability profile after treatment with ASOs **A1–A6**. Mice (BalbC, $n = 4$/group) were dosed s.c. with 0.5, 1.0, 5.0 and 25.0 mg/kg of ASOs **A1–A4**, 5.0 and 25.0 mg/kg of ASO **A5** and 1.0 and 25.0 mg/kg of ASO **A6**, twice a week for 3 weeks and animals were sacrificed 48 h after last dose. Organs were harvested and SR-B1 mRNA was quantified by qRT–PCR and normalized to the saline-treated group. The 0.5 mg/kg dose group for ASO **A4** was not counted in the final analysis due to a dosing error. SR-B1 mRNA reduction in (**A**) liver (**B**) quadriceps and (**C**) heart. Plasma levels post sacrifice for (**D**) ALT. Organ weights for (**E**) liver (**F**) spleen. Plasma levels post-sacrifice for (**G**) cholesterol and (**H**) triglycerides. Error bars indicate ±standard deviation.

plasma cholesterol levels of the treated mice. The high-dose ASO-treated group showed between 3- and 5-fold increases in plasma cholesterol levels (Figure 2G) relative to saline which were consistent with the expected phamacological response for reducing SR-B1 gene expression. In contrast, there were no noticiable effects on the levels of plasma triglycerides (Figure 2H) indicating that the increase in plasma cholesterol levels were indeed

related to SR-B1 down-regulation. In general, all the ASOs were well-tolerated with no elevations in transaminase levels (ALT) and liver weights (Figure 2D and E). Slight elevations in spleen weights were observed for the high-dose group ASO **A1**-treated mice although these could be, in part, related to the pharmacological effects of the ASO or to the lack of 5-Me groups on the cytosine nucleobases in the tcDNA-modified ASOs (Figure 2F). 5-Me groups on the deoxycytidine nucleobase are known to mitigate the immune stimulation properties of CpG oligonucleotides (35).

To ascertain if tcDNA 14-mers were generally less active as compared to 14-mer ASOs with other higher affinity modifications in the wings, we evaluated a 14-mer tcDNA ASO **A7** targeting mouse phosphatase and tensin homologue (PTEN) and compared it to a 14-mer LNA benchmark ASO **A8** (Supplementary Figure S6). This sequence has been used extensively by us to profile the antisense properties of ASOs modified with various BNA and HNA analogs (13–17). We found that the tc-DNA 14-mer showed lower T_m and reduced activity in cell culture and in the animal experiment as compared to the LNA benchmark ASO. However, unlike the LNA ASO **A8**, the tcDNA ASO did not show elevations in ALT levels for the high-dose group-treated animals.

We also quantified the level of ASOs **A1–A6** in liver tissue (Supplementary Figure S7). Consistent with previous studies of PS-modified gapmer ASOs, drug accumulation in liver was dependent on dose and the overall PS content of the ASO. Thus, both the 20-mer ASOs **A1** and **A5** showed very similar levels of accumulation at the 25 and 5 mg/kg dose. However, the effect of wing chemistry on tissue accumulation was more evident for the shorter tcDNA ASOs which showed higher drug levels in liver tissue. For example, the16-mer and 18-mer tcDNA ASOs **A2** and **A3** showed similar liver accumulation as the 20-mer ASOs **A1** and **A6** but the 14-mer tcDNA ASO **A4** showed almost 3-fold higher accumulation in liver tissue as compared to the 14-mer cEt ASO **A6**. It is possible that the more hydrophobic nature of the tcDNA monomers enhances binding to plasma proteins but this effect is most prominent for shorter ASOs as compared to the longer designs where increased PS content dominates ASO distribution.

To further understand ASO distribution between different cell types in the liver and kidney, we stained tissue sections from mice treated with the 20-mer tcDNA and MOE ASOs **A1** and **A5**, respectively, and 14-mer cEt ASO **A6** using a rabbit polyclonal antibody raised against the MOE ASO **A5** (Supplementary Figure S8). We found no qualitative changes in ASO distribution between the different cell types in the liver but darker staining for oligonucleotide was observed in the non-parenchymal cells of the liver for all the ASOs evaluated. However, the differential recognition of the antibody for ASOs **A1**, **A5** and **A6** does not allow for any quantitative estimation of changes in sub-organ distribution to be made at this point.

To confirm the observations from the first study and to examine the effect of the ASO treatment on SR-B1 mRNA down-regulation in tissues other than liver, heart and quadriceps, we carried out a follow-up study (Figure 3). Mice ($n = 4$/group) were injected s.c. with ASOs **A1–A6** formulated in saline at 25 mg/kg twice a week for 3 weeks. Animals were sacrified 48 h after the last ASO dose and down-regulation of SR-B1 mRNA in liver, kidney, diaphragm, lung, fat, heart, quadriceps and gastrocnemius was measured by quatitative RT-PCR and the results were normalized to saline-treated animals (Figure 3A). As seen in the previous study, we observed >95% down-regulation of the SR-B1 mRNA for all the ASO-treated groups in liver tissue. In kidney, ASOs **A1–A3** and **A6** showed similar activity for reducing SR-B1 mRNA while **A4** and **A5** were less active. A similar trend was observed in lung tissue while in the diaphragm all but ASO **A4** showed similar activity. In fat, heart, quadriceps and gastrocnemius, the tcDNA ASOs **A1–A4** showed activity directly propotional to ASO length. The 14-mer cEt ASO **A6** showed activity comparable to the 20-mer tcDNA **A1** in all the tissues evaluated. Once again, all the ASOs were well-tolerated with no elevations in plasma ALT (Figure 3B) or organ weights (Figure 3C–E).

DISCUSSION

Our evaluation of tcDNA gapmer ASOs presents several interesting observations. When combined with the phosphorothioate backbone modification, tcDNA gapmer ASOs show similar to slightly improved duplex thermal stability relative to length-matched MOE gapmer ASO but reduced thermostability relative to length-matched cEt or LNA gapmer ASOs. This observation is generally in line with the duplex stabilizing properties reported for these modifications in oligonucleotide sequences used for biophysical studies. In cell culture, tcDNA ASOs showed activity which was consistent with their duplex thermostability measurements under transfection and free-uptake conditions. For example, the 20-mer tcDNA and MOE ASOs **A1** and **A5**, respectively, showed the highest T_m and best activity for reducing SR-B1 mRNA in cell culture followed by the 18-mer **A2**, 16-mer **A3** and 14-mer **A4** tcDNA ASOs. In general, the T_m and cell culture observations were recapitulated in the animal experiments where the 20-mer tcDNA and MOE ASOs **A1** and **A5**, respectively, exhibited better activity relative to the 18-mer, 16-mer and 14-mer tcDNA ASOs **A2**, **A3** and **A4**. However, somewhat surprisingly, the shorter 14-mer cEt ASO **A6** showed the best overall activity in the animal experiments despite lower T_m and ~5-fold reduced potency relative to the 20-mer tcDNA and MOE ASOs **A1** and **A5**, respectively, in cell culture. The 14-mer cEt ASO **A6** also showed ~3-fold improved activity in cell culture as compared to 16-mer tcDNA ASO **A3** even though both ASOs had identical RNA-binding affinity. Moreover, improved activity in animal experiments was observed despite reduced overall liver accumulation for the 14-mer cEt ASO **A6**. ASOs, unlike small molecules drugs, cannot distribute to all the different cellular compartments by passive diffusion. ASOs are known to enter cells via multiple pathways some of

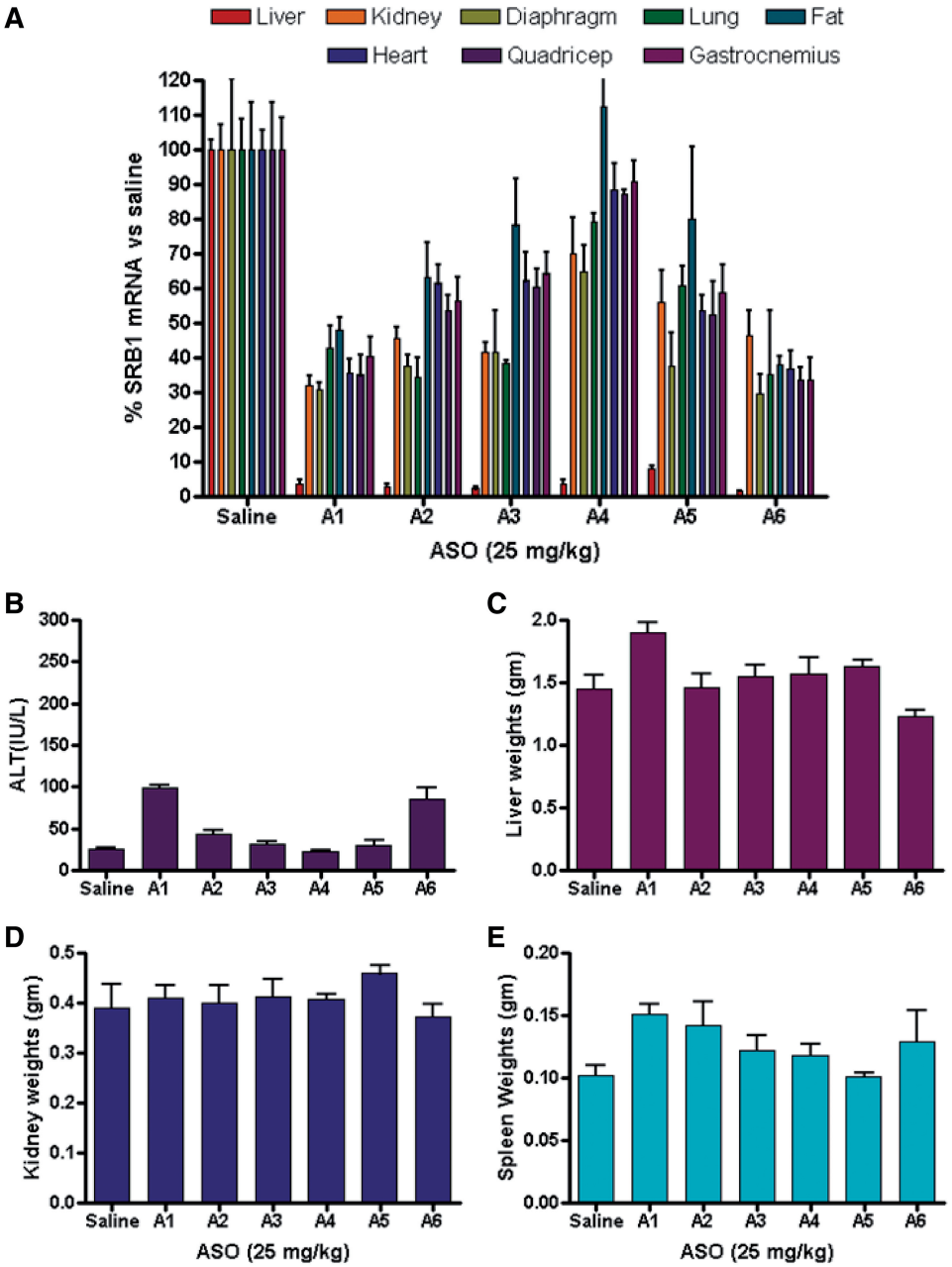

Figure 3. Reduction of SR-B1 mRNA and tolerability profile after treatment with ASOs **A1–A6**. Mice (BalbC, $n = 4$/group) were dosed s.c. with 25.0 mg/kg of ASOs **A1–A6**, twice a week for 3 weeks and animals were sacrificed 48 h after last dose. Organs were harvested and SR-B1 mRNA in was quantified by qRT–PCR and normalized to the saline-treated group. SR-B1 mRNA reduction in (**A**) liver, kidney, diaphragm, lung, fat, heart, quadriceps and gastrocnemius. Plasma levels post-sacrifice for (**B**) ALT. Organ weights for (**C**) liver, (**D**) kidney and (**E**) spleen. Error bars indicate ± standard deviation.

which are productive and lead to sequence specific gene down-regulation of the targeted mRNA in the nucleus (21,36). In contrast, non-productive pathways lead to ASO accumulation into endosomal and lysosomal compartment where they are most likely metabolized by nuclease-mediated digestion and excreted. It is also known that phosphorothioate-modified single-stranded ASOs interact with several proteins within the cell some of which might be responsible for differential trafficking of the ASO to different sub-cellular compartments leading to different pharmacological and toxicological properties (21,36). It is possible that ASO length and chemical modification can have a differential impact on these interactions resulting in the observed effects. Another interesting result from this study was the robust antisense activity seen in multiple tissues with several of the ASOs evaluated. Perhaps, more importantly, these effects were observed in the absence of elevated plasma transaminases indicating that it is possible to achieve robust antisense effects in tissues other than liver without producing hepatoxicity. Thus, our data show that phosphorothioate-modified gapmer ASOs can down-regulate gene

expression in a therapeutically relevant manner in hepatic and extra-hepatic tissues and this can be further modulated by ASO length and wing chemistry.

CONCLUSIONS

In conclusion, we show for the first time that tcDNA phosphorothioate-modified gapmer ASOs show robust antisense effects for reducing gene expression in multiple tissues without producing hepatotoxicity. With the exception of the cEt ASO **A6**, all ASOs evaluated showed activity consistent with their T_m and cell culture profile. The origins of the improved potency despite lower T_m, cell culture activity and reduced tissue exposure observed with the cEt ASO **A6** in liver are not properly understood as of yet. However, they are likely related to differential sub-cellular ASO distribution which is in turn influenced by ASO length and specific structural features of the modified nucleotides in the flanks of the ASO. Our data provides an impetus to further explore phosphorothioate-modified tcDNA and related modifications for therapeutic antisense applications using the RNase H and other antisense mechanisms.

SUPPLEMENTARY DATA

Supplementary Data are available at NAR Online: Supplementary Table 1 and Supplementary Figures 1–8.

ACKNOWLEDGEMENTS

We thank Dr Hans Gaus and Dr Balkrishen Bhat for helpful discussions and Dr Gene Hung for the histology analysis.

FUNDING

Funding for open access charge: Isis Pharmaceuticals.

Conflict of interest statement. None declared.

REFERENCES

1. Bennett,C.F. and Swayze,E.E. (2010) RNA targeting therapeutics: molecular mechanisms of antisense oligonucleotides as a therapeutic platform. *Annu. Rev. Pharmacol. Toxicol.*, **50**, 259–293.
2. Raal,F.J., Santos,R.D., Blom,D.J., Marais,A.D., Charng,M.J., Cromwell,W.C., Lachmann,R.H., Gaudet,D., Tan,J.L., Chasan-Taber,S. *et al.* (2010) Mipomersen, an apolipoprotein B synthesis inhibitor, for lowering of LDL cholesterol concentrations in patients with homozygous familial hypercholesterolaemia: a randomised, double-blind, placebo-controlled trial. *Lancet*, **375**, 998–1006.
3. Lares,M.R., Rossi,J.J. and Ouellet,D.L. (2010) RNAi and small interfering RNAs in human disease therapeutic applications. *Trends Biotechnol.*, **28**, 570–579.
4. Krutzfeldt,J., Rajewsky,N., Braich,R., Rajeev,K.G., Tuschl,T., Manoharan,M. and Stoffel,M. (2005) Silencing of microRNAs in vivo with 'antagomirs'. *Nature*, **43**, 685–689.
5. Elmen,J., Lindow,M., Schutz,S., Lawrence,M., Petri,A., Obad,S., Lindholm,M., Hedtjarn,M., Hansen,H.F., Berger,U. *et al.* (2008) LNA-mediated microRNA silencing in non-human primates. *Nature*, **452**, 896–899.
6. Steffy,K., Allerson,C. and Bhat,B. (2011) Perspectives in MicroRNA therapeutics. *Pharm. Technol.*, **s18**, s20–s22, s24.
7. Swayze,E.E. and Bhat,B. (2008) The Medicinal Chemistry of Oligonucleotides. In: Crooke,S.T. (ed.), *Antisense Drug Technology: Principles, Strategies, and Applications*, 2nd edn. CRC Press, Boca Raton, pp. 143–182.
8. Prakash,T.P. and Bhat,B. (2007) 2'-Modified oligonucleotides for antisense therapeutics. *Curr. Top. Med. Chem.*, **7**, 641–649.
9. Veedu,R.N. and Wengel,J. (2010) Locked nucleic acids: promising nucleic acid analogs for therapeutic applications. *Chem. Biodivers.*, **7**, 536–542.
10. Herdewijn,P. (2010) Nucleic acids with a six-membered carbohydrate' mimic in the backbone. *Chem. Biodiversity*, **7**, 1–59.
11. Leumann,C.J. (2002) DNA analogues: from supramolecular principles to biological properties. *Bioorg. Med. Chem.*, **10**, 841–854.
12. Monia,B.P., Lesnik,E.A., Gonzalez,C., Lima,W.F., McGee,D., Guinosso,C.J., Kawasaki,A.M., Cook,P.D. and Freier,S.M. (1993) Evaluation of 2'-modified oligonucleotides containing 2'-deoxy gaps as antisense inhibitors of gene expression. *J. Biol. Chem.*, **268**, 14514–14522.
13. Seth,P.P., Siwkowski,A., Allerson,C.R., Vasquez,G., Lee,S., Prakash,T.P., Wancewicz,E.V., Witchell,D. and Swayze,E.E. (2009) Short antisense oligonucleotides with novel 2'-4' conformationaly restricted nucleoside analogues show improved potency without increased toxicity in animals. *J. Med. Chem.*, **52**, 10–13.
14. Seth,P.P., Allerson,C.R., Berdeja,A., Siwkowski,A., Pallan,P.S., Gaus,H., Prakash,T.P., Watt,A.T., Egli,M. and Swayze,E.E. (2010) An exocyclic methylene group acts as a bioisostere of the 2'-oxygen atom in LNA. *J. Am. Chem. Soc.*, **132**, 14942–14950.
15. Seth,P.P., Allerson,C.R., Siwkowski,A., Vasquez,G., Berdeja,A., Migawa,M.T., Gaus,H., Prakash,T.P., Bhat,B. and Swayze,E.E. (2010) Configuration of the 5′-methyl group modulates the biophysical and biological properties of locked nucleic acid (LNA) oligonucleotides. *J. Med. Chem.*, **53**, 8309–8318.
16. Prakash,T.P., Siwkowski,A., Allerson,C.R., Migawa,M.T., Lee,S., Gaus,H.J., Black,C., Seth,P.P., Swayze,E.E. and Bhat,B. (2010) Antisense oligonucleotides containing conformationally constrained 2',4'-(N-methoxy)aminomethylene and 2',4'-aminooxymethylene and 2'-O,4'-C-aminomethylene bridged nucleoside analogues show improved potency in animal models. *J. Med. Chem.*, **53**, 1636–1650.
17. Egli,M., Pallan,P.S., Allerson,C.R., Prakash,T.P., Berdeja,A., Yu,J., Lee,S., Watt,A., Gaus,H., Bhat,B. *et al.* (2011) Synthesis, improved antisense activity and structural rationale for the divergent RNA affinities of 3′-fluoro hexitol nucleic acid (FHNA and ara-FHNA) modified oligonucleotides. *J. Am. Chem. Soc.*, **133**, 16642–16649.
18. Renneberg,D. and Leumann,C.J. (2002) Watson-Crick base-pairing properties of tricyclo-DNA. *J. Am. Chem. Soc.*, **124**, 5993–6002.
19. Ittig,D., Liu,S., Renneberg,D., Schumperli,D. and Leumann,C.J. (2004) Nuclear antisense effects in cyclophilin A pre-mRNA splicing by oligonucleotides: a comparison of tricyclo-DNA with LNA. *Nucleic Acids Res.*, **32**, 346–353.
20. Seth,P.P., Vasquez,G., Allerson,C.A., Berdeja,A., Gaus,H., Kinberger,G.A., Prakash,T.P., Migawa,M.T., Bhat,B. and Swayze,E.E. (2010) Synthesis and biophysical evaluation of 2',4'-constrained 2'O-methoxyethyl and 2',4'-constrained 2'O-ethyl nucleic acid analogues. *J. Org. Chem.*, **75**, 1569–1581.
21. Koller,E., Vincent,T.M., Chappell,A., De,S., Manoharan,M. and Bennett,C.F. (2011) Mechanisms of single-stranded phosphorothioate modified antisense oligonucleotide accumulation in hepatocytes. *Nucleic Acids Res.*, **39**, 4795–4807.
22. Dean,N.M., McKay,R., Condon,T.P. and Bennett,C.F. (1994) Inhibition of protein kinase C-alpha expression in human A549 cells by antisense oligonucleotides inhibits induction of intercellular adhesion molecule 1 (ICAM-1) mRNA by phorbol esters. *J. Biol. Chem.*, **269**, 16416–16424.

23. Dean,N.M. and Griffey,R.H. (1997) Identification and characterization of second-generation antisense oligonucleotides. *Antisense Nucleic Acid Drug Dev.*, **7**, 229–233.
24. Altmann,K.H., Martin,P., Dean,N.M. and Monia,B.P. (1997) Second generation antisense oligonucleotides - inhibition of pkc-alpha and c-raf kinase expression by chimeric oligonucleotides incorporating 6'-substituted carbocyclic nucleosides and 2'-*O*-ethylene glycol substituted ribonucleosides. *Nucleosides Nucleotides Nucleic Acids*, **16**, 917–926.
25. Teplova,M., Minasov,G., Tereshko,V., Inamati,G.B., Cook,P.D., Manoharan,M. and Egli,M. (1999) Crystal structure and improved antisense properties of 2'-*O*-(2-methoxyethyl)-RNA. *Nat. Struct. Biol.*, **6**, 535–539.
26. Martin,P. (2003) Ein neuer Zugang zu 2'-O-(2-Methoxyethyl)ribonucleosiden ausgehend von D-Glucose *Helv. Chim. Acta*, **86**, 204.
27. Geary,R.S., Yu,R.Z. and Levin,A.A. (2001) Pharmacokinetics of phosphorothioate antisense oligodeoxynucleotides. *Curr. Opin. Invest. Drugs*, **2**, 562–573.
28. Straarup,E.M., Fisker,N., Hedtjarn,M., Lindholm,M.W., Rosenbohm,C., Aarup,V., Hansen,H.F., Orum,H., Hansen,J.B. and Koch,T. (2010) Short locked nucleic acid antisense oligonucleotides potently reduce apolipoprotein B mRNA and serum cholesterol in mice and non-human primates. *Nucleic Acids Res.*, **38**, 7100–7111.
29. Ittig,D., Gerber,A.-B. and Leumann,C.J. (2010) Position-dependent effects on stability in tricyclo-DNA modified oligonucleotide duplexes. *Nucleic Acids Res.*, **39**, 373–380.
30. Acton,S., Rigotti,A., Landschulz,K.T., Xu,S., Hobbs,H.H. and Krieger,M. (1996) Identification of scavenger receptor SR-BI as a high density lipoprotein receptor. *Science*, **271**, 518–520.
31. Bartosch,B., Vitelli,A., Granier,C., Goujon,C., Dubuisson,J., Pascale,S., Scarselli,E., Cortese,R., Nicosia,A. and Cosset,F.-L. (2003) Cell entry of hepatitis C virus requires a set of co-receptors that include the CD81 tetraspanin and the SR-B1 scavenger receptor. *J. Biol. Chem.*, **278**, 41624–41630.
32. Rodrigues,C.D., Hannus,M., Prudencio,M., Martin,C., Goncalves,L.A., Portugal,S., Epiphanio,S., Akinc,A., Hadwiger,P., Jahn-Hofmann,K. *et al.* (2008) Host scavenger receptor SR-BI plays a dual role in the establishment of malaria parasite liver infection. *Cell Host Microbe*, **4**, 271–282.
33. Freier,S.M., Alkema,D., Sinclair,A., Neilson,T. and Turner,D.H. (1985) Contributions of dangling end stacking and terminal base-pair formation to the stabilities of XGGCCp, XCCGGp, XGGCCYp, and XCCGGYp helixes. *Biochemistry*, **24**, 4533–4539.
34. Freier,S.M. and Altmann,K.H. (1997) The ups and downs of nucleic acid duplex stability: structure-stability studies on chemically-modified DNA:RNA duplexes. *Nucleic Acids Res.*, **25**, 4429–4443.
35. Krieg,A.M. (1999) Mechanisms and applications of immune stimulatory CpG oligodeoxynucleotides. *Biochim. Biophys. Acta*, **1489**, 107–116.
36. Geary,R.S., Wancewicz,E., Matson,J., Pearce,M., Siwkowski,A., Swayze,E. and Bennett,F. (2009) Effect of dose and plasma concentration on liver uptake and pharmacologic activity of a 2'-methoxyethyl modified chimeric antisense oligonucleotide targeting PTEN. *Biochem. Pharmacol.*, **78**, 284–291.